CPC(HEP & NP), 2009, **33**(11): 935—943 **Chinese Physics C** Vol. 33, No. 11, Nov., 2009

In-situ monitoring of $EuTiO_3$ and $SrTiO_3$ film growth using time-resolved X-ray scattering during pulsed-laser deposition

WANG Huan-Hua(王焕华)[1)]

(Institute of High Energy Physics, Chinese Academy of Sciences, Beijing 100049, China)

Abstract Time-resolved X-ray scattering was employed to in-situ monitor the epitaxial growth process of the thin films and multilayers of $EuTiO_3$ and $SrTiO_3$ during pulsed laser deposition. The temporal intensity oscillations of the reflected X-rays at anti-Bragg position and the transient processes following the flux pulses were observed. The temporal intensity oscillations were used to control the film thickness, and the reflectivity along the crystal truncation rod was used to measure both the film thickness and the surface/interface roughness. The primary features of the X-ray intensity oscillations were reproduced via simulating the experimental data using diffusive rate equation model. Several mechanisms of determining the X-ray intensity features were discerned.

Key words time-resolved X-ray scattering, PLD, $EuTiO_3$, $SrTiO_3$, thin film, multilayer

PACS 61.10.Eq, 61.10.Kw, 81.15.Fg, 68.55.-a, 68.55.Jk

1 Introduction

Thin crystalline film growth is the basis of today's microelectronics industry and information technology, which are based on the well-developed thin film technologies of semiconductors and metals. In contrast to this situation, the growth techniques of complex multi-component functional oxides (ferroelectric, ferromagnetic, colossal magnetoresistance, superconducting, etc.) are still not mature enough for large-scale practical applications[1]. For example, high temperature superconducting electronic devices based on trilayer Josephson junctions are still not practical due to the unavailability of atomic-scale smooth abrupt surface/interface of high T_c cuprites (e.g. $Yba_2Cu_3O_{7-\delta}$). Before their growth mode is mediated from three-dimensional into two-dimensional and thus atomic-scale surface flatness is achieved, their industrial applications based on multi-layered heterostructures seem not optimistic.

Two-dimensional (layer-by-layer or step-flow) growth is preferred for getting a smooth, thin, and continuous film. However, in practical situations, the material to be used cannot always be chosen so that layer-by-layer or step-flow growth is favored. How to mediate the growth process to get the preferred layer-by-layer growth mode is still not clear. Therefore, a thorough understanding of the mechanisms involved in the epitaxial growth of complex materials at atomic scale must be achieved first, which is not only of fundamental interest, but also of technological importance. For this purpose, we constructed a state-of-art facility by combining the time-resolved X-rays scattering (TRXRS) with the pulsed laser deposition (PLD) in the G3 experimental station at the Cornell High Energy Synchrotron Source (CHESS), which enables us to carry out studies on the growth process of complex oxide thin films and heterostructures.

Although enormous efforts have been made to study the growth mechanism of complex oxides in PLD, our understanding is still far from thorough. This is not only because it is a difficult far-from-equilibrium process, but also because the growth process is further complicated by many influencing factors, such as a lattice mismatch between substrate and film, oxygen pressure, substrate temperature, kinetic energy of the incident flux, and so on. To simplify the growth process and data analysis, we have

---

Received 17 December 2008, Revised 31 March 2009

[1)] E-mail: wanghh@ihep.ac.cn Fax:86-10-88236229; Tel: 86-10-88235994 successfully decoupled the intrinsic growth mechanism from strain effect by using an ideal strain-free system: $EuTiO_3$ (ETO) film on $SrTiO_3$ (STO) substrate[2]. Our focus is to study the surface processing during PLD growth of ETO and STO thin films by combining TRXRS measurements with model calculations, especially to investigate the effects of kinetic energy of the incident flux particles on the growth process.

In this report, we measured the TRXRS and the fluorescence during the growth of ETO and STO films. The temporal intensity oscillations of reflected X-rays were used to control the film thickness during the growth of $(STO)_m/(ETO)_n$ multilayers. The crystal truncation rods (CTR) were measured for calculating the film thickness and surface/interface roughness. In order to understand the TRXRS data, we simulated the intensity oscillations of the reflected X-rays as well as those of the reflection high-energy electron diffraction (RHEED) for comparison.

2 Experiment

The growth of ETO and STO thin films was monitored using the PLD/TRXRS facility at CHESS. In these experiments, the STO (001) substrate sat at the original of an X-ray diffractometer whose motions were integral components of the PLD growth chamber.

The STO target was commercially provided, and the ETO targets were synthesized as previously described[2]. Carefully cleaned STO (001) substrates were fixed to the heater with clamps without additional surface preparation. The target-substrate distance was 6.8 cm. A pulsed excimer laser (Lambda Physik, 248 nm) was focused on one of the rotating targets. During the depositions oxygen pressure was controlled dynamically at a set level.

In situ X-ray measurements of the growth process were performed. First, at the growth temperature we found and located the detector at the anti-Bragg position (001/2) of STO substrate. Then we started to grow thin film and collected X-ray scattering data simultaneously. At the anti-Bragg position, destructive interference occurs and maximum sensitivity of TRXRS to the variation in surface structure is achieved. Specially, the time dependence of the scattered X-ray intensity at the anti-Bragg condition (equivalent to the out-of-phase condition in RHEED) exhibits intensity oscillations as the film grows. These oscillations can be caused both by variations in the surface roughness during layer-by-layer growth (as in RHEED studies) and by interference between X-rays reflected by the thin film surface and the film-substrate interface (Kiessig fringes)[3]. This later effect is only present in heteroepitaxy, and is not usually observable in RHEED studies. The time-dependences of the Eu $L_{2,3}$ fluorescent emission lines were simultaneously monitored using a multi-channel analyzer (MCA), providing an independent in situ measurement of the thickness of the ETO film[4, 5]. During the growth, the deposition could be interrupted for measuring the CTR, from which the film thickness and the surface roughness can be calculated.

After deposition, the film was cooled down to room temperature under the same oxygen pressure. The as-grown films of both ETO and STO were optically transparent. The surface morphology of the samples was examined using tapping mode atomic force microscopy (AFM).

3 Results and discussion

3.1 Growth of ETO thin films

The two-dimensional growth mode of ETO thin film is layer-by-layer in a very wide growth temperature range and a wide growth rate range, as shown in Fig. 1 and Fig. 2(a). Fig. 1 indicates that the temperature variation in this range from 650 ℃ to 100 ℃ did not significantly affect the growth mode. Similarly, in Fig. 2(a), the oscillations were not affected with varying the laser repetition rate from 0.1 Hz to 10 Hz at 650 ℃. So ETO is an excellent material for fundamental studies on layer-by-layer growth processing of complex oxides.

Figure 1 also reveals two other features. As the laser was off at $t = 1650$ second, the reflected X-ray intensity started to decay, and once the laser was back on, the intensity oscillations recovered, indicating the surface was roughening during the non-deposition hiatus. At 550 ℃, the growth was interrupted at the minimum B and the maximum T of an oscillation cycle, and the reflections along the CTR were immediately measured. The corresponding Kiessig fringes were shown in the two insets. Obviously, the minimum B and the maximum T of the temporal intensity oscillation cycle correspond to the bottom and the peak at anti-Bragg position ($Q = 0.5$) in the Kiessig fringes, respectively. It infers that the temporal intensity oscillations of specularly reflected X-ray beam arise from film thickness variation, rather than from periodic variations in surface roughness.

The quantitative relationship between the film thickness and the temporal intensity oscillations was obtained via measuring the reflectivity along the CTR after interrupting the growth. Fig. 2(b) shows the Kiessig fringes immediately measured after the interruptions at 16th, 21st, 26th, and 33rd oscillation cycle in Fig. 2(a). The reflectivity curves were fitted using Parratt32 software. Table 1 shows the fitting results (the error bar represents a doubling of χ^2). The lattice constant c of ETO was assumed to be 3.93 Å at 600 ℃ for calculating the corresponding monolayer (ML) number. Clearly, the difference of ML numbers between neighboring interruptions is approximately 2 times the difference of the corresponding oscillation cycle numbers, indicating each oscillation cycle corresponds to 2 ML. But the absolute thickness values by these two methods have a larger discrepancy. So besides the fitting error, there exist other error sources. One is that we tried to interrupt the deposition right at the oscillation maxima or minima to get an integral number of monolayers, but in fact the intensity extrema do not coincide with the integer monolayers if the surface height distribution is asymmetric[4]. Another source is that the time scan of the X-ray intensity and the laser firing are manually controlled in these experiments, thus they were not simultaneously started, interrupted, recovered and ended. So the higher the laser repetition rate was, the larger this error was, as shown in Fig. 2.

The CTR measurements also give the surface roughness. As shown in Table 1, the root-mean-square (rms) roughness of a substrate at different stages is different due to the fitting error. We need to mention that we did not subtract the backgrounds from the reflectivity curves, therefore the measured roughness value is a little smaller than it actually is.

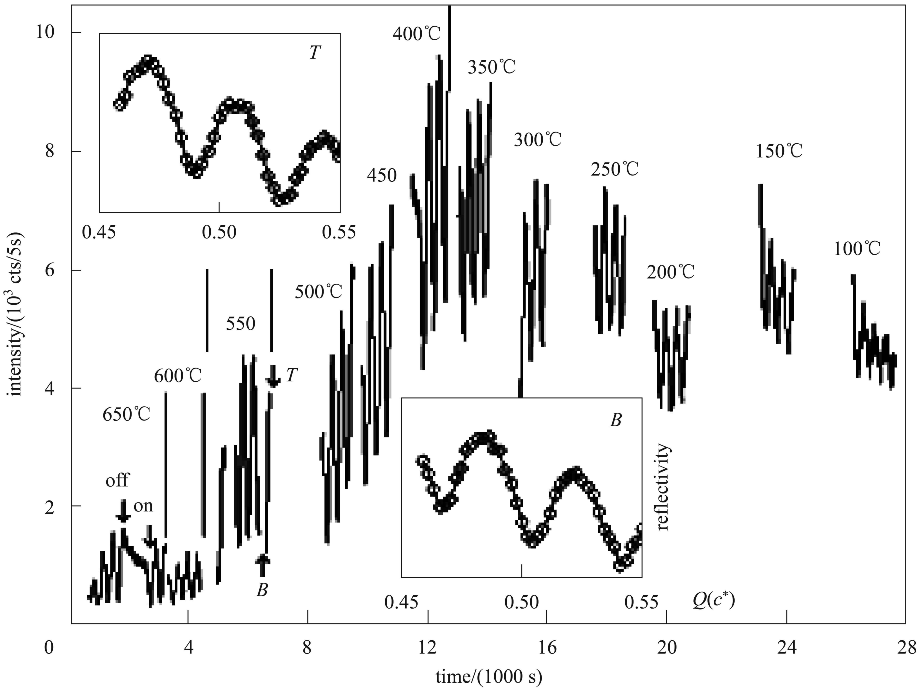

Fig. 1. Evolution of specularly reflected X-rays intensity at the anti-Bragg position during PLD growth of ETO on STO (001) with varying the heater temperature from 650 ℃ to 100 ℃. Kiessig fringes measured at B and T are plotted in the insets, with the ordinate and abscissa being the reflectivity and the scattering vector $Q(c^*)$, respectively.

Table 1. Fitting results of Fig. 2(b) (Suppose c = 3.93 Å at 600 ℃).

Osc.#	thickness by Osc. (ML)	thickness by fitting		film/substrate rms roughness/Å
		(ML)	/Å	
16	32	33.25±0.15	130.69±0.60	0/2.933
21	42	44.36±0.15	174.33±0.58	0/2.566
26	52	52.26±0.17	205.39±0.67	0/3.018
33	66	66.39±0.18	260.92±0.70	0/2.383

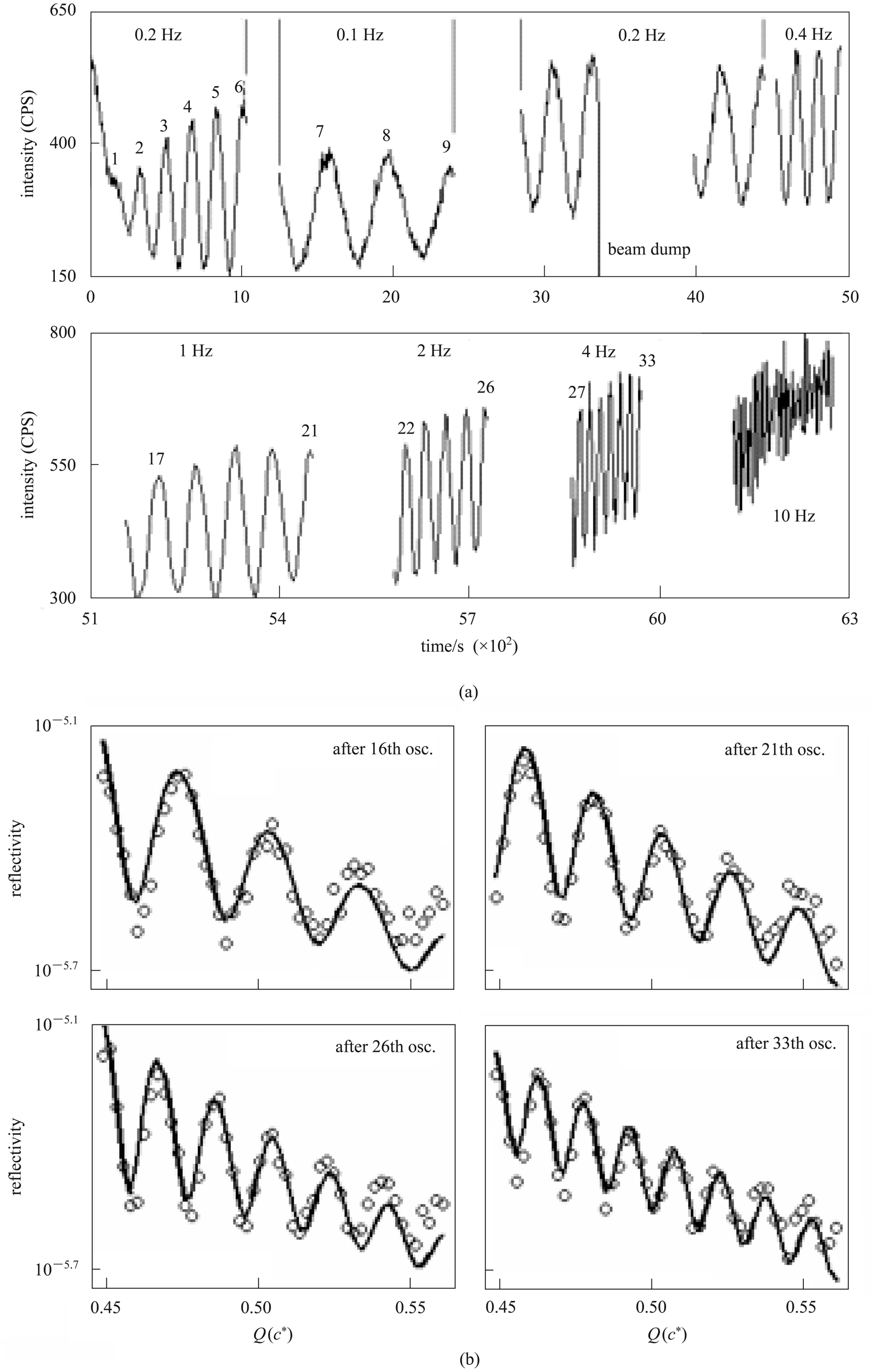

Fig. 2. (a) X-rays specular reflection intensity oscillations at the anti-Bragg position during growth of ETO on STO (001) at 600 ℃ with varying laser pulse repetition from 0.1 Hz to 10 Hz. (b) Kiessig fringes measured (open dots) after 16, 21, 26, and 33 oscillation cycles, respectively, and their fitting curves (solid lines).

The oscillations due to periodic variation in coverage of top layers (equally, variation in surface roughness) will appear only when the substrate is very flat and the growth front consists of less than three incomplete monolayers, as revealed in the following model calculations. Fig. 3 shows the modulated X-ray intensity oscillations resulting not only from the increasing of ETO film thickness but also from the cyclical variation in coverage.

In these experiments, each laser pulse adds only about 1/42 ML, so the corresponding change of the reflected X-ray intensity is so small that the oscillation curve looks continuous. However, since PLD is an intermittent growth process, where the periodic bursts of highly driven growth are followed by relatively long periods of uninterrupted surface relaxation, a transient process following a pulse of deposition flux does exist and can be measured. Fig. 4 shows the temporal intensity oscillations and the averaged steps and transient processes over all phases in the insets. Here all the transient processes were averaged in order to suppress the noise. The X-ray intensity recovery rate in the transient process is actually oscillation phase dependent, as demonstrated in the following model calculation results as well as in Ref. [6].

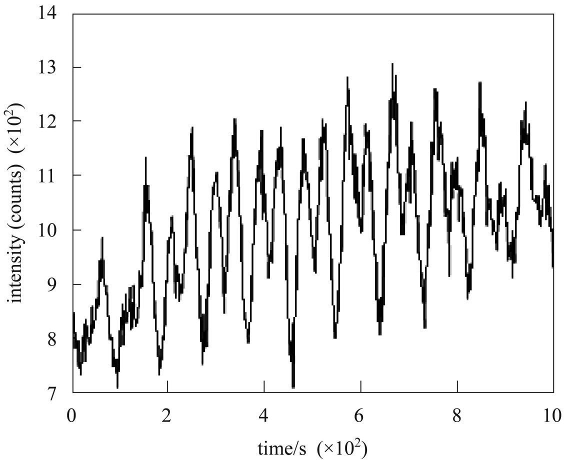

Fig. 3. X-ray intensity oscillations arising both from film thickness increasing and from cyclic roughness variations during the growth of ETO thin film on STO substrate.

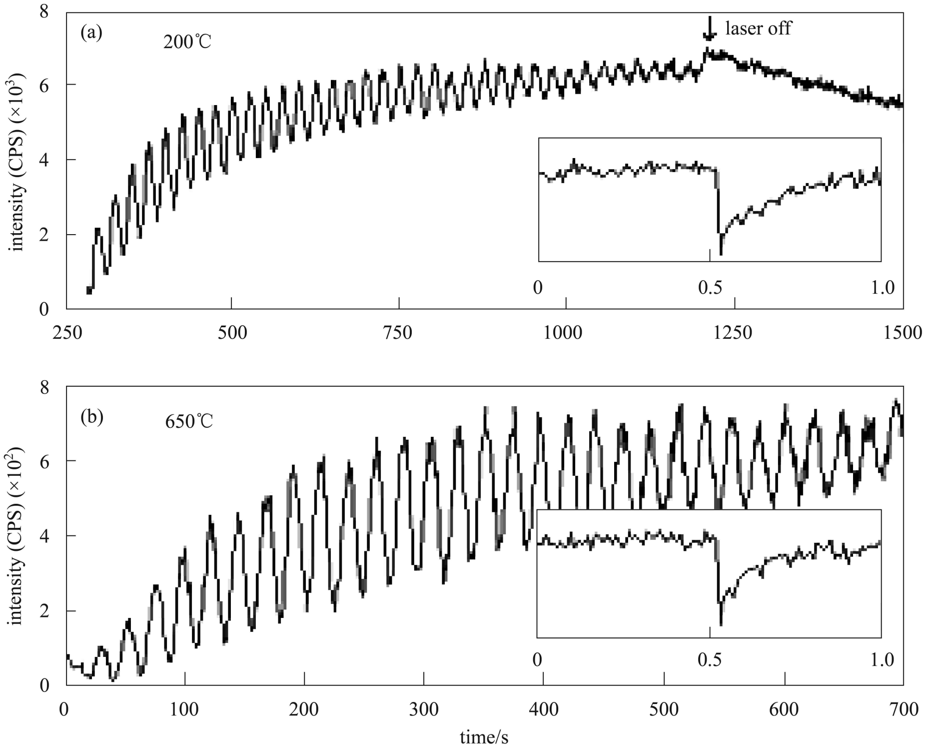

Fig. 4. X-rays specular reflection oscillations at the anti-Bragg position and the averaged transient processes followed a material flux deposition with growth conditions: 7×10^{-6} torr, 1 Hz, 8 J/cm^2, and (a) 200 ℃, (b) 650 ℃, respectively.

3.2 Growth of STO thin films

Figure 5 displays various features of the XRS intensity oscillations during STO growth. The primary features of these curves can be reproduced in the calculations using diffusive rate equation model, which provides a bridge between the experiments data and our understanding of the mechanisms involved in the growth. In Fig. 5(a), after the initial nucleation and coalesce, the oscillation amplitude increases first, because the growth smoothens the substrate surface, and then decreases while the background increases, because the roughness is accumulating. In Fig. 5(b), the oscillation amplitude does not change obviously after the initial growth, but the background increases significantly, which is mainly due to the nonuniformity of the growth rate over the area sampled by X-ray beams. In Fig. 5(c), the oscillation amplitude firstly increases and then decays while the background firstly increases significantly and then saturates, meaning that the initial growth smoothens the film surface but the roughness accumulates quickly. Fig. 5(d) shows a section of the non-damping intensity oscillations without obvious changes in the amplitude and the background, indicating a steady growth with nearly constant growth front.

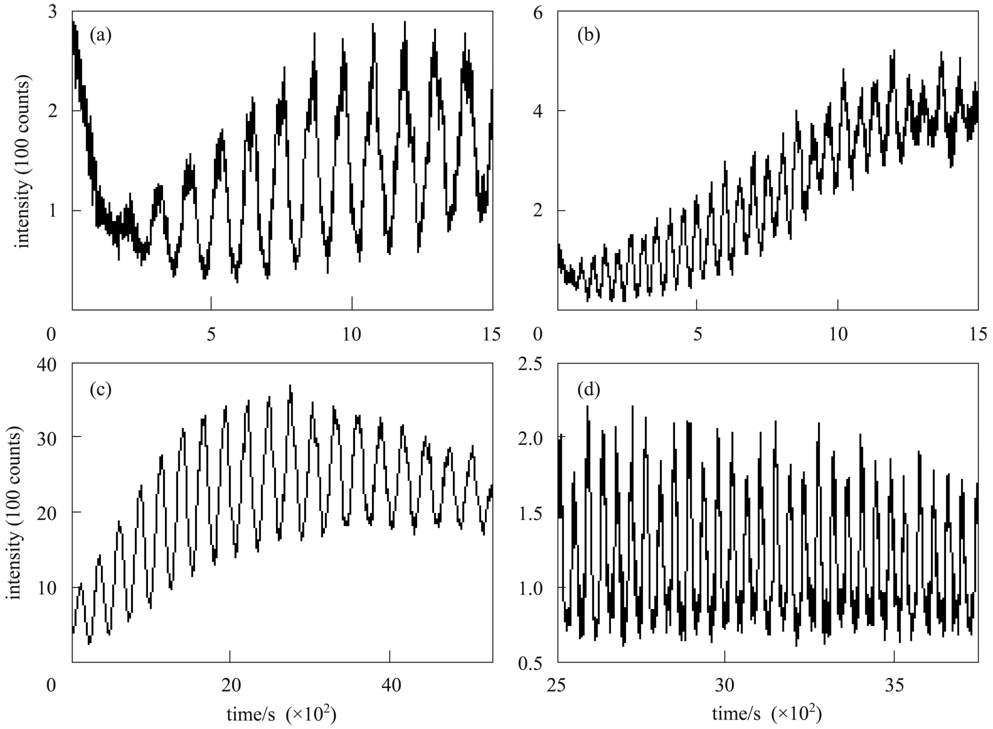

Fig. 5. X-rays intensity oscillations during the growth of STO on STO (001) with growth conditions: (a) 650 ℃, 7×10^{-6} torr, 0.25 Hz, 3 J/cm^2; (b) 710 ℃, 12.4 mtorr, 1 Hz, 23 J/cm^2; (c) 650 ℃, 7×10^{-6} torr, 1 Hz, 10 J/cm^2; and (d) 710 ℃, 12.4 mtorr, 1 Hz, 23 J/cm^2.

During the interruption of the growth process of STO thin film, Kiessig fringes were also measured, indicating that it actually is not a real homoeptiaxial growth due to the formation of oxygen-vacancy in the film when growing under low oxygen pressures and at high growth temperatures[7, 8]. So here the intensity oscillations arose only from the film thickness increase.

3.3 Growth of ETO/STO multilayers

ETO and STO layers can epitaxially grow on each other in a layer-by-layer growth manner. Fig. 6 plots the time dependence of the specularly reflected X-rays intensity (upper) and the Eu Kα fluorescence intensity (lower) simultaneously obtained during the growth of ETO/STO multilayers. We can accurately control the thickness of the STO and ETO sublayers using the X-ray intensity oscillations. A TEM image confirmed the sublayer thickness in this heterostructure.

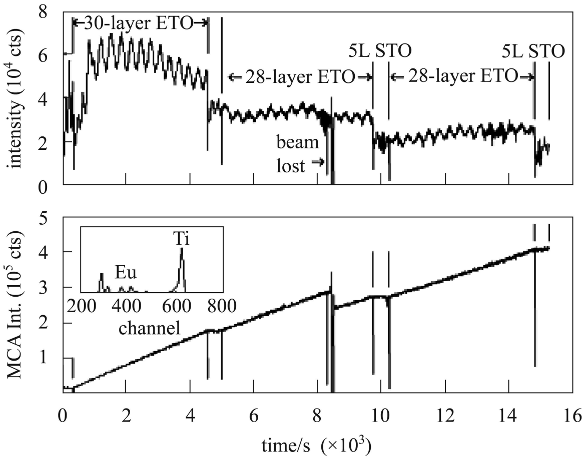

Fig. 6. (a) X-rays reflection and (b) X-ray fluorescence simultaneously measured during the growth of STO/ETO multilayers at 650 ℃, 0.7 mTorr, 0.2 Hz and 3 J/cm^2. The initial 3 oscillation cycles arose from $SrTiO_3$ homoepitaxial growth.

The integrated intensity of Eu Kα fluorescence emission increases linearly with time during the deposition of ETO sublayers, and keeps constant during the deposition of STO sublayers. Since X-ray absorption is negligible for the film thickness studied in this measurement, the intensity of the Eu Kα fluorescence X-rays is directly proportional to the amount of Eu deposited on the surface, so the growth rate of ETO can be obtained from the X-ray fluorescence-versus-time curve after calibrating the X-ray fluorescence intensity with film thickness.

4 Theoretical interpretations

For comparison, TRXRS and RHEED intensity behaviors were calculated together. In RHEED, the strong dynamical interaction between probe and sample restricts the sampling to the outmost layers, making this probe only sensitive to variation in coverage of topmost layers. So RHEED intensity has no oscillations except the transient in step-flow growth where the surface roughness is self-similar and not periodically varied[9]. For X-rays, a kinematic theory accurately describes the scattering and allows quantitative interpretation of scattered intensity. Because X-rays penetrate deeply into matter, they can sample all scatters both in thin film and in substrate, thus buried layer thickness and surface/interface roughness can be measured. So a notable point is that this technique can be used to control the thickness no matter whether the growth mode is layer-by-layer or step-flow, while RHEED can be used only for layer-by-layer mode.

We used Cohen's rate equation model of diffusive growth[10] to show the behaviors of RHEED and TRXRS during thin film growth. To make the mathematics simple, several assumptions were made: (1) The diffusion parameter k is the same for all interlayer diffusions; (2) Only "downhill" mass diffusion happens. (3) Only the diffusions between neighboring atomic layers are considered. The equation and boundary conditions are

$$\begin{aligned}\mathrm{d}\theta_n/\mathrm{d}t &= (1/\tau)(\theta_{n-1}-\theta_n)+\\ &\quad k(\theta_{n+1}-\theta_{n+2})(\theta_{n-1}-\theta_n)-\\ &\quad k(\theta_n-\theta_{n+1})(\theta_{n-2}-\theta_{n-1})\\ \theta_0(t) &= 1\\ \theta_n(0) &= 0\end{aligned}$$

where $\theta_n(t)$ is the coverage function of the nth monolayer at time t, and τ is the time needed to grow 1 ML. The equation was solved using numerical computation of Runge-Kutta method.

For simplicity, the RHEED intensity is assumed to come from only the top exposed layers. So the electron diffraction amplitude and intensity at anti-Bragg position are

$$A_{\mathrm{ETO}}=F_{\mathrm{ETO}}\sum_{n=0}^{20}(\theta_n-\theta_{n+1})\exp(\mathrm{i}n\pi),$$

$$I_{\mathrm{RHEED}}=|A_{\mathrm{ETO}}|^2.$$

For X-rays intensity, the contributions of all monolayers must be included. Take r_0 to denote Thomson scattering length and c the lattice constant. So $N=1/c^2$, being the number of lattice points in unit area. At $\vec{q}=(001/2)c^*$, the X-ray amplitudes scattered from the substrate and from the film are

$$\begin{aligned}A_{\mathrm{STO}}(\vec{q}) &= -r_0\sum_{R_n}\exp(\mathrm{i}\vec{q}\cdot\vec{R}_n)\sum_{r_j}f_j\exp(\mathrm{i}\vec{q}\cdot\vec{r}_j)=\\ &\quad -\frac{1}{2}r_0NF_{\mathrm{STO}},\\ A_{\mathrm{ETO}}(\vec{q}) &= -r_0\sum_{\vec{R}_n}\exp(\mathrm{i}\vec{q}\cdot\vec{R}_n)\sum_{\vec{r}_j}f_j\exp(\mathrm{i}\vec{q}\cdot\vec{r}_j)=\\ &\quad -r_0NF_{\mathrm{ETO}}\sum_{Z=na}\theta_n\exp(\mathrm{i}\pi n),\end{aligned}$$

$$I_{\mathrm{xray}}=|A_{\mathrm{ETO}}+A_{\mathrm{STO}}|^2.$$

In order to discern the factors that determine the primary features of the observed intensity oscillations, various situations from the simplest to the much more complicated ones were calculated (ignore the constant prefactors).

The simplest situation is the continuous growth of ETO films on ideally flat STO substrates (represented by the topmost coverage equals 1) with constant growth rate. As shown in Fig. 7, the X-ray intensity oscillations arising from both the thickness increase and the cyclic roughness variation appear only when the simultaneously growing monolayers are less than three. The oscillations caused by roughness variation disappear when the growth front consists of more than three incomplete monolayers. With weak interlayer diffusion (k is small), the roughness increases with time, so does the background. This figure also conforms that the intensity maxima and minima do not coincide with integral numbers of monolayers when the surface becomes rougher.

Considering more complicated situations where the substrate is rough and the growth rate is nonuniform over the sampled area, calculations reproduced the primary features of the intensity oscillation curves observed in the experiments. Compared with flat substrate, rough substrate increases the oscillation background and decreases the oscillation amplitude. The spacial ununiformity of growth rate further enhance these trends, because it increases the phase difference of the growth processes on widely separated regions of the probed area by X-ray beam.

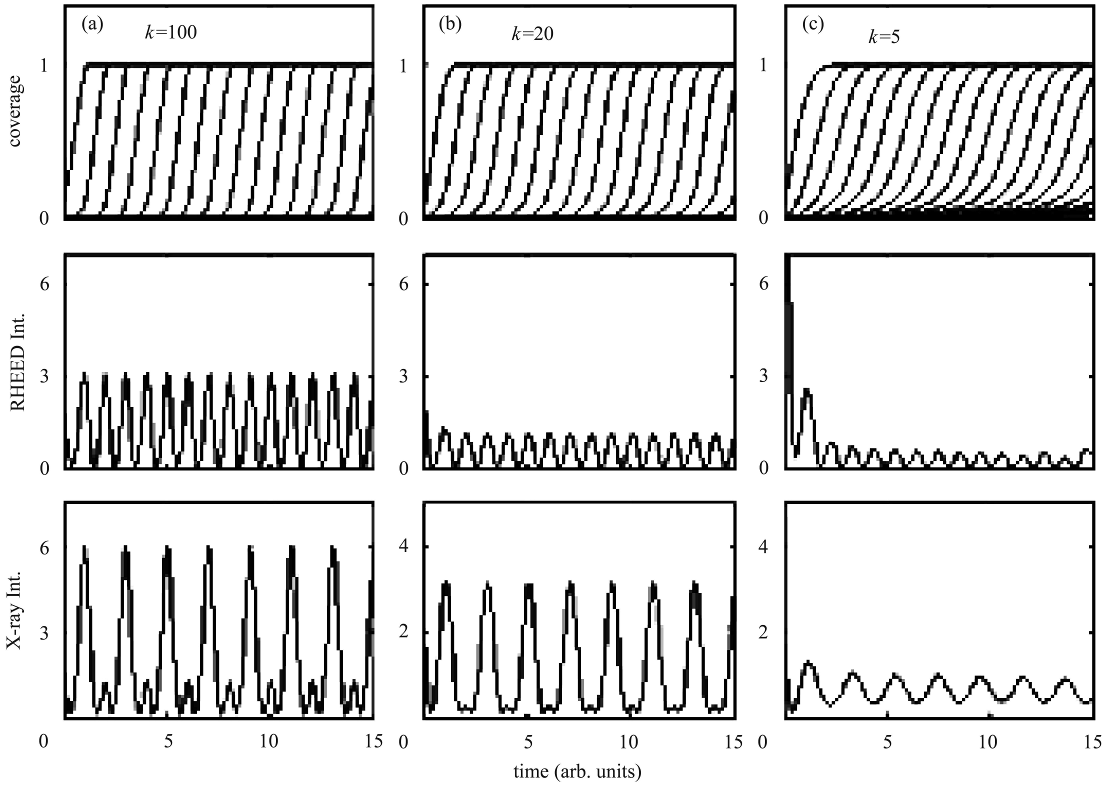

Fig. 7. The calculated coverage and the corresponding RHEED and X-ray intensities at anti-Bragg position during continuous growth of ETO film on ideally flat STO substrates with the diffusion parameter (a) k=100, (b) k=20, and (c) k=5, respectively.

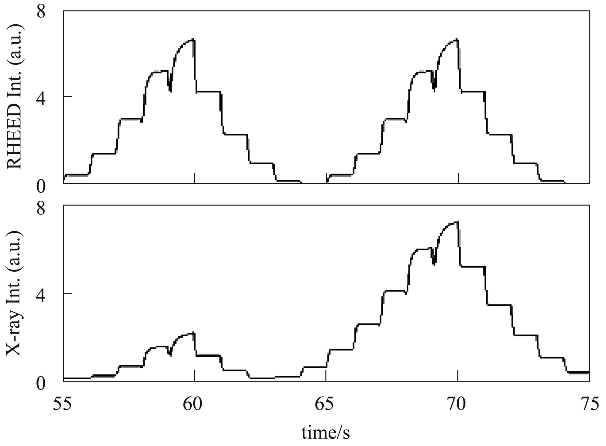

Fig. 8. The calculated RHEED and X-ray intensity oscillations during intermittent growth of ETO film on flat STO substrate with k=40. The transient processes are displayed.

The above calculation results based on continuous growth are closed to experimental observations because each laser pulse adds only ~1/42 ML in the experiments. If the pulsed flux is large enough (e.g. 0.1 L/pulse), intensity steps and transient processes following each laser pulse would appear, as shown in Fig. 8, which is quite similar to the averaged ones in Fig. 4. This behavior was also observed in other experiments using RHEED[9] and TRXRS[11].

5 Conclusion

In summary, we have illustrated the feasibility of combining time-resolved X-ray scattering with model calculation to understand the PLD growth processes of complex oxides. Time-resolved X-ray scattering enables in-situ real-time monitoring the growth processes of thin films and multilayers of ETO and STO. The growth phases, transient process, growth rate, film thickness and surface morphology can be measured and quantitatively analyzed due to the applicability of kinematical theory. The primary features of the time-resolved X-ray scattering intensity oscillations can be understood according to diffusive rate equation model calculations.

The experimental part was based on the data obtained at Cornell High Energy Synchrotron Source four years ago. Dr. Aaron Fleet, Dr. Darren Dale, Professor Yuri Suzuki and Professor Joel Brock are acknowledged for their work or discussions for these experiments. Data analysis and most of model calculation were performed at Beijing Synchrotron Radiation Laboratory, Institute of High Energy Physics, Chinese Academy of Sciences.

References

1 WILLMOTT P R. Progress in Surface Science, 2004, **76**: 163
2 WANG Huan-Hua, FLEET Aaron, BROCK Joel D et al. J. Appl. Phys., 2004, **96**(9): 5324
3 Als-Nielsen J, McMorrow D. Elements of Modern X-ray Physics. New York: Wiley, 2001
4 HEADRICK R L, KYCIA S, WOLL A R et al. Phys. Rev. B, 1998, **58**: 4818
5 HEADRICK R L, KYCIA S, PARK Y K et al. Phys. Rev. B, 1995, **54**: 14686
6 FLEET A, DALE D, SUZUKI Y et al. Phys. Rev. Lett., 2005, **94**: 036102
7 NISHIMURA T, IKEDA A, NAMBA H et al. Surf. Sci., 1999, **421**: 273
8 ZEGENHAGEN J, HAAGE T, JIANG Q D. Appl. Phys. A: Matter. Sci. Proc., 1998, **67**: 711
9 LIPPMAA M, NAKAGAWA N, KAWASAKI M et al. Appl. Phys. Lett., 2000, **76**: 2439
10 COHEN P I, Petrich G S, Pukite P R et al. Surf. Sci., 1989, **216**: 222
11 ERES G, TISCHLER J Z, YOON M et al. Appl. Phys. Lett., 2002, **80**: 3379